Hindawi Publishing Corporation
International Journal of Photoenergy
Volume 2016, Article ID 3129896, 5 pages
http://dx.doi.org/10.1155/2016/3129896

Research Article

Aluminum-Doped SnO_2 Hollow Microspheres as Photoanode Materials for Dye-Sensitized Solar Cells

Binghua Xu, Zeng Chen, and Shengjun Li

Key Laboratory of Photovoltaic Materials of Henan Province and School of Physics & Electronic, Henan University, Kaifeng 475001, China

Correspondence should be addressed to Shengjun Li; lishengjun1011@126.com

Received 21 March 2016; Revised 5 May 2016; Accepted 17 May 2016

Academic Editor: Germà Garcia-Belmonte

Al doped SnO_2 microspheres were prepared through hydrothermal method. As-prepared SnO_2 microspheres were applied as photoanode materials in dye-sensitized solar cells (DSCs). The properties of the assembled DSCs were significantly improved, especially the open-circuit voltage. The reason for the enhancement was explored through the investigation of dark current curves and electrochemistry impedance spectra. These results showed that the Al doping significantly increased the reaction resistance of recombination reactions and restrained the dark current. The efficient lifetime of photoexcited electrons was also obviously lengthened.

1. Introduction

Dye-sensitized solar cells (DSCs) have been actually promoted by the development of nanocrystal materials, especially the preparation of TiO_2 nanocrystals with different morphology [1, 2]. High photoelectric conversion efficiency up to 14.3% has been obtained [3]. However, the band gap of TiO_2 is about 3.2 eV which causes obvious catalyzing properties under UV light. The organic solvent in DSCs might be slightly decomposed by TiO_2 nanoparticles on the photoanode under sunlight. As an alternative to TiO_2, SnO_2 has been extensively investigated as a photoanode material in DSCs. SnO_2 has a wider band gap (about 3.6 eV) than that of TiO_2 which was inactive to the organic solvent in DSCs. And SnO_2 has high electron mobility (about 150 $cm^2V^{-1}s^{-1}$) which is a benefit for the collection of the photoexcited electrons in the photoanode [4, 5]. However, the band edge of conduction band edge of SnO_2 is −4.5 eV (vacuum level) which causes serious back reaction between the electrons in the conduction band and the oxide ions in the electrolyte. It is an efficient way to inhibit these back reactions by doping SnO_2 with other metal elements. Duan et al. doped SnO_2 nanoparticle with Al and found the tuning of the conduction band and suppression of charge recombination [6]. Li et al. prepared Zn-doped SnO_2 nanocrystals to obtain longer electron lifetimes and higher dye loading [7].

In this work, we prepared Al doped SnO_2 hollow microspheres. The electron recombination was efficiently restrained and the photoelectrical conversion efficiency was significantly enhanced compared with that of pure SnO_2.

2. Experimental

2.1. Preparation of Pure SnO_2 Power and Al Doped SnO_2 Power. SnO_2 microspheres were synthesized using the hydrothermal method as follows. For the preparation of SnO_2 power, 0.8 g of stannous chloride dihydrate ($SnCl_2{\cdot}2H_2O$) was dissolved in 80 mL deionized water. *D*-Glucose was used as the soft template. The content of *D*-glucose was 7.024 g. The former mixture was stirred for 30 min. at room temperature. The resulting well-distributed mixture was transferred into a 100 mL autoclave for hydrothermal reaction at 180°C. The hydrothermal reaction time was 16 h. After the autoclave was cooled to room temperature, the product was collected by centrifugation and washed with distilled water and ethanol several times. The obtained sample was dried at 60°C overnight. The resulting brown power was calcined at 550°C for 1 h in air to obtain the final product. For preparing the

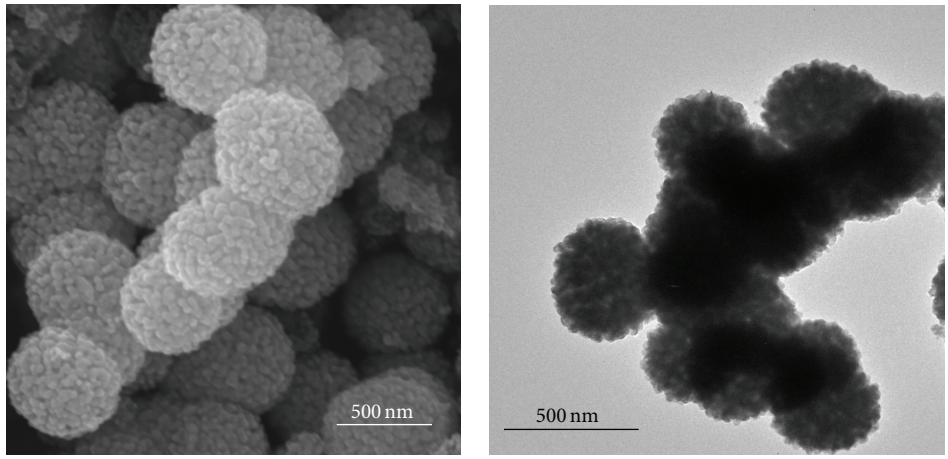

(a) (b)

Figure 1: SEM (a) and TEM (b) of SnO_2 hollow microspheres doped with 1.5% Al.

Al doped SnO_2 sample, aluminum(III) chloride ($AlCl_3$) was added to the precursor solution. The addition amount of Al was controlled to be 0.5%, 1.0%, 1.5%, and 2.0% (at%) of Sn content in the solution. The preparation processes of Al doped SnO_2 power were controlled to be the same as that described above except for the addition of $AlCl_3$. The obtained samples of pure SnO_2 and Al doped SnO_2 powder were denoted as pure SnO_2, 0.5% Al doped SnO_2, 1.0% Al doped SnO_2, 1.5% Al doped SnO_2, and 2.0% Al doped SnO_2, respectively.

2.2. Fabrication of DSSC Based on Pure SnO_2 and Al Doped SnO_2. To prepare the working electrode, SnO_2 or Al doped SnO_2 slurry was covered on fluorine-doped tin oxide (FTO) glass ($1 \times 2\ cm^2$, $15\ \Omega sq^{-1}$, Opvtech) using a doctor blade technique and then sintered at 450°C for 30 min. After cooling to 80°C, the samples were immersed in 5×10^{-4} mol L^{-1} ethanol of N719 dye for 24 h. Pt counter electrode was prepared by spreading 5 mM H_2PtCl_6 aqueous solution on an FTO glass substrate, followed by pyrolyzation at 390°C for 15 min. The mixture of 0.6 M dimethylpropylimidazolium iodide, 0.1 M iodine, 0.5 M 4-*tert*-butylpyridine, and 0.1 M lithium iodide in methoxyacetonitrile was prepared as the electrolyte of DSCs.

2.3. Characterization and Optical Measurements. The crystalline phase of the samples was characterized by DX-2700 X-ray diffractometer (XRD) with monochromatized Cu K irradiation. The morphology was studied using a JSM-7001F field emission scanning electron microscope (FE-SEM) and JEM 2100 transmission electron microscope (TEM). XPS measurements were performed in Thermo Scientific ESCALAB 250 station (Thermo Fisher Scientific, Massachusetts, USA). Photocurrent density-voltage (J-V) characteristics were measured using a Keithley 2440 Source Meter under AM 1.5 G illumination from a Newport Oriel Solar Simulator with an intensity of one sun. The incident light intensity was calibrated with a standard Si solar cell provided by Newport Oriel. The active cell area of the assembled DSCs was $0.25\ cm^2$. An electrochemistry workstation (IM6) was used to investigate the electrochemical impedance spectra (EIS) of DSCs. This measurement was also carried out with the same structured DSCs as that used in the former experiments. The impedance measurement of DSCs was recorded under dark condition at the bias potential of −0.6 V over a frequency range of 0.1–1 MHz with an AC amplitude of 10 mV.

3. Results and Discussion

Figure 1(a) shows the morphology of the prepared Al doping SnO_2 microspheres. The diameter is 300–500 nm. These SnO_2 microspheres were piled up with homogeneous nanoparticles. The size of the particles is 20–40 nm. There are some broken microspheres which indicate that the prepared SnO_2 is hollow microspheres. This structure is a benefit for the absorbing of dye and the diffusion of the electrolyte in DSCs. TEM was also carried out to confirm the hollow spheres structure of SnO_2. The TEM of SnO_2 microspheres is shown in Figure 1(b). The whole SnO_2 spheres show almost the same darkness which indicates that the thickness at the center of SnO_2 spheres is almost the same as that of edge. Therefore, the as-prepared SnO_2 should be hollow spheres.

Figure 2 shows the XRD spectra of SnO_2 microspheres doped with different Al content. The prepared SnO_2 microspheres correspond to the cassiterite structured SnO_2 (JCPDS database card number 41-1445). There is almost no change in the XRD spectra with the addition of Al element which might be because the content of added Al element is too little to change the structure of SnO_2. The crystalline particle size (D) could be estimated from the 110, 101, and 211 diffraction peak using the Scherrer equation [8]:

$$D = \frac{0.89\lambda}{\beta \cos\theta}, \quad (1)$$

where λ is the wavelength of the X-ray, β is the full-width at half-maximum (FWHM), and θ is the Bragg angle in the

Table 1: Detailed photovoltaic parameters of the DSCs based on the SnO_2 hollow microspheres doped with different Al content.

Al content/at%	V_{OC} mV	J_{SC}/mA cm^{-2}	FF/%	Efficiency/%
0	179	8.05	32.2	0.46
0.5	347	9.40	51.7	1.69
1.0	412	10.71	53.4	2.36
1.5	474	11.48	55.8	3.04
2.0	442	9.56	55.2	2.34

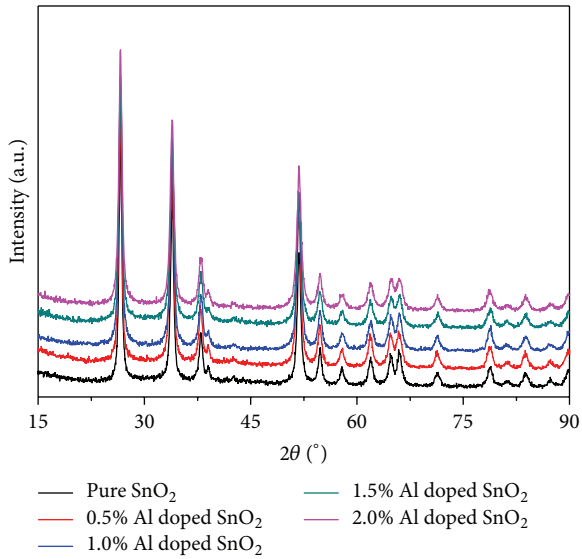

Figure 2: XRD of SnO_2 hollow microspheres doped with different Al content.

diffraction pattern. The particle size was estimated to be about 17.0 nm for Al doped SnO_2.

XPS were carried out to confirm the introduction of Al into the SnO_2 hollow spheres. The survey scan spectra and the element narrow scan of 1.5% (at%) Al doped SnO_2 are shown in Figure 3. The XPS of pure hollow microspheres were shown in the insert of the corresponding spectra. The binding energies of O 1s and Sn 3d show no obvious shift after Al doping. However, a new weak peak appears at about 75 eV which corresponds to Al 2p. The content of Al was also estimated to be about 0.61% (at%). The content of Al is so little that the O 1s and Sn 3d have no change which is in accordance with the result of XRD.

Figure 4(a) shows the J-V curves of the DSCs assembled with Al doped SnO_2 microspheres photoanode. The specific parameters of these J-V curves were summarized in Table 1. The photoanode prepared with pure SnO_2 microspheres shows low open-circuit voltage (V_{OC}, 179 mV) due to the low conduction band edge. V_{OC} increased from 179 mV to 474 mV when the addition of Al increased from 0 to 1.5% (at%). At the same time, the short circuit current density (J_{SC}) was also enhanced significantly from 8.05 mA cm^{-2} to 11.48 mA cm^{-2}. The photoelectric conversion efficiency (η) increased from 0.46% to 3.04%. However, V_{OC} and J_{SC} both decreased when the addition of Al further increased to 2.0% (at%). The increase of V_{OC} should be due to the inhibition of back reaction after the doping of Al. Figure 4(b) shows the dark current-voltage curves. The dark current density becomes weaker and weaker with the increase of Al doping content. The depression of dark current should be one key reason for the increase of V_{OC}.

Electrochemical impedance spectroscopy (EIS) is an efficient method to investigate the recombination process of the photoexcited electrons. EIS was carried out on the SnO_2 and Al doped SnO_2 under dark condition. The bias potential is −0.6 V. The Nyquist plots are shown in Figure 5(a). The Nyquist plots were fitted using the equivalent circuit shown in the insert of Figure 5(a). In the equivalent circuit, R_S represent the series resistors during the transport of electrons. R_{ct1} correspond to the resistance during the charge-transfer processes occurring at the counter electrode/electrolyte interface. R_{ct2} should correspond to the recombination of electron at the SnO_2/electrolyte interface. From the fitting result of Nyquist plots, it can be seen that R_S and R_{ct1} show few changes before and after Al doping. However, R_{ct2} increases from 35 Ω cm^{-2} to 127 Ω cm^{-2} after Al doping. This indicates that the photoelectron recombination is efficiently inhibited. Figure 5(b) shows the Bode phase plots of the pure SnO_2 sphere film and the Al (1.5%, at%). There are two electrochemical processes, ω_1 and ω_2, which occur at high frequency (10^3 Hz–10^5 Hz) and low frequency (1 Hz to 10^3 Hz), respectively. ω_1 corresponds to the charge-transfer processes occurring at the counter electrode/electrolyte interface [9, 10]. ω_2 should correspond to the charge-transfer processes occurring at the SnO_2/electrolyte interface. The characteristic frequency of ω_2 may reflect the electron lifetimes (τ_e) of the injected electrons [11]. The lifetimes (τ_e) of the photoexcited electron in the photoanodes were determined using the following equation:

$$\tau_e = \frac{1}{2\pi f_{max}}. \quad (2)$$

The characteristic frequencies of these photoanodes, SnO_2 and Al doped SnO_2, are 3.1 and 1.2 Hz, respectively. According to (2), the electron lifetimes (τ_e) were calculated to be about 51 ms and 132 ms for the SnO_2 and Al doped SnO_2 electrodes, respectively. It can be seen that Al doping can enhance the efficient electron lifetime of SnO_2 electrodes. This result is in accordance with that of dark current experiments (shown in Figure 4).

4. Conclusions

Al doped SnO_2 microspheres were prepared through hydrothermal method using glucose as template. The SnO_2 microspheres were piled up with SnO_2 nanoparticles. As-prepared SnO_2 microspheres were applied as photoanode materials in dye-sensitized solar cells. The results showed that the Al doping significantly restrained the dark current and improved the open-circuit voltage of the cells. Electrochemistry impedance spectra showed that the reaction resistance of recombination reactions increased sharply after doping of Al and the efficient

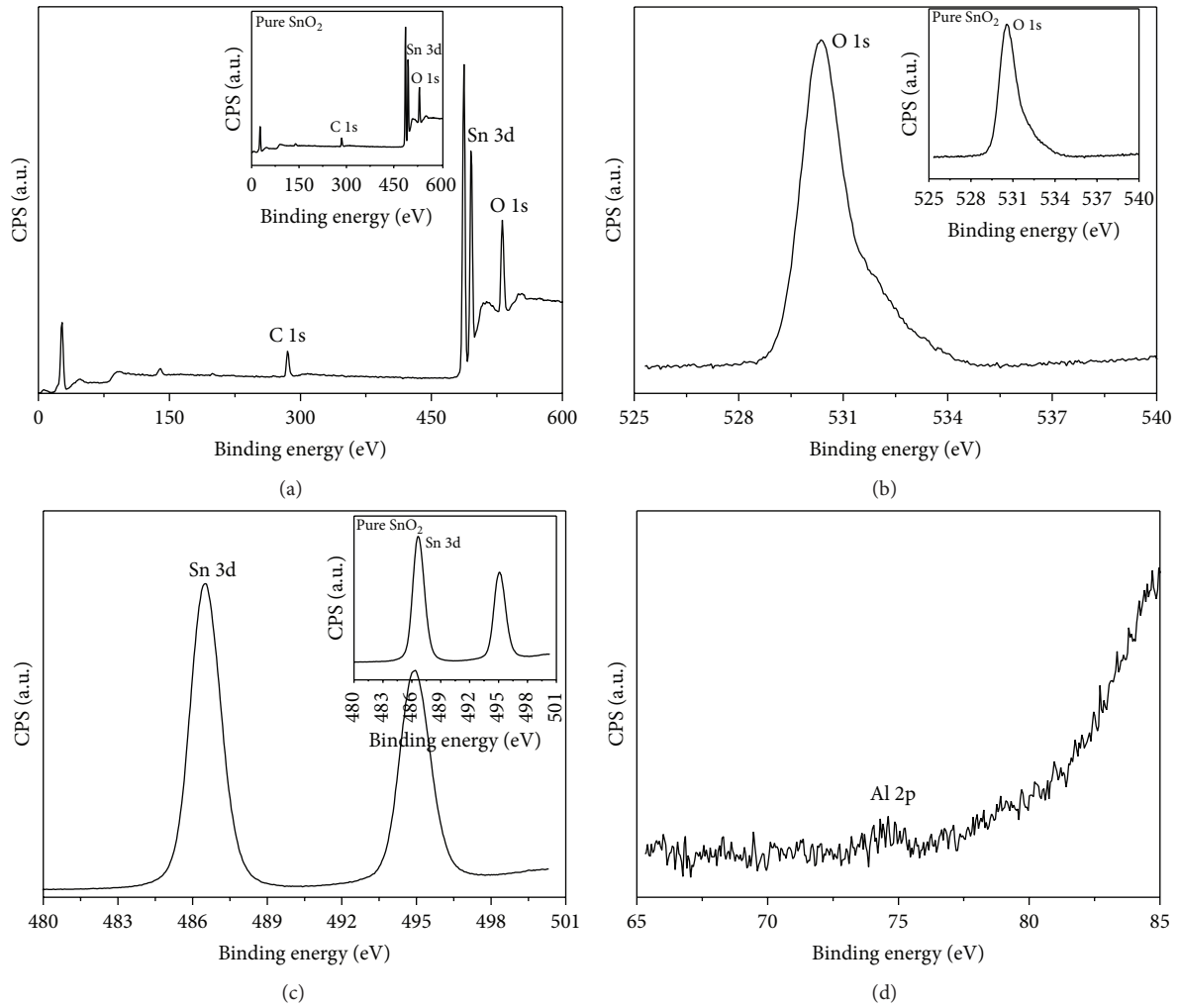

FIGURE 3: XPS of SnO_2 hollow microspheres doped with 1.5% Al and pure SnO_2 hollow microspheres (given in the insert): (a) full spectra; (b) high resolution of O 1s; (c) high resolution of Sn 3d; (d) high resolution of Al 2p.

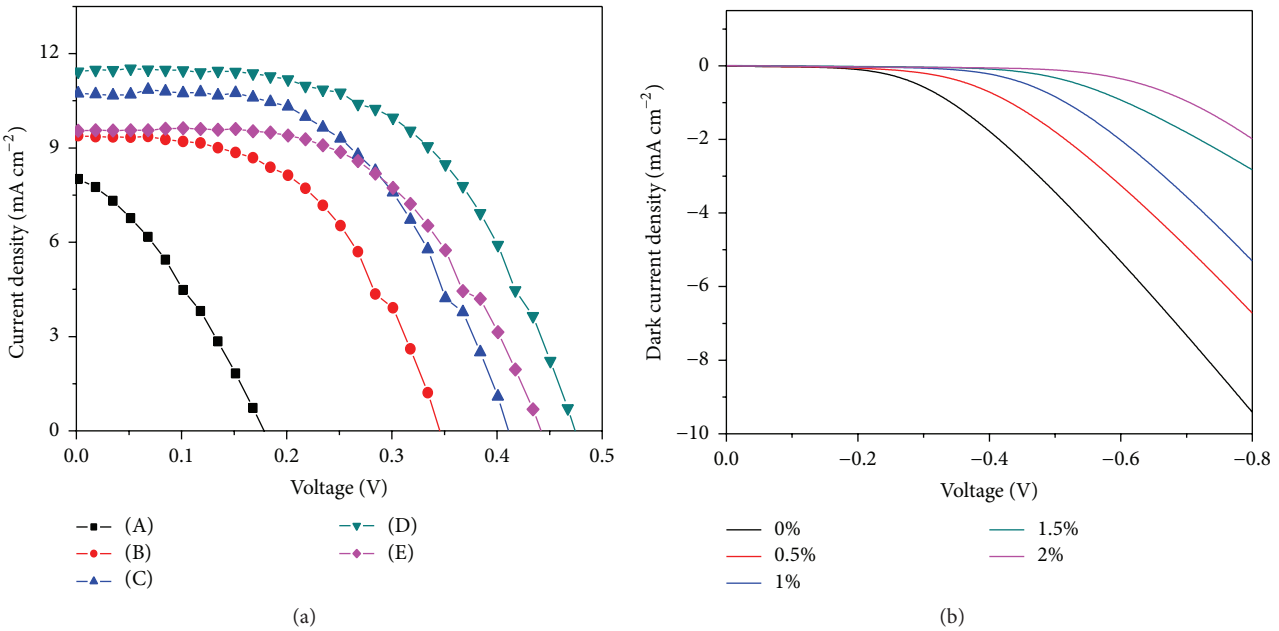

FIGURE 4: *J-V* characteristic of the DSCs based on the SnO_2 hollow microspheres doped with different Al content (a) and the corresponding dark current-voltage curves (b).

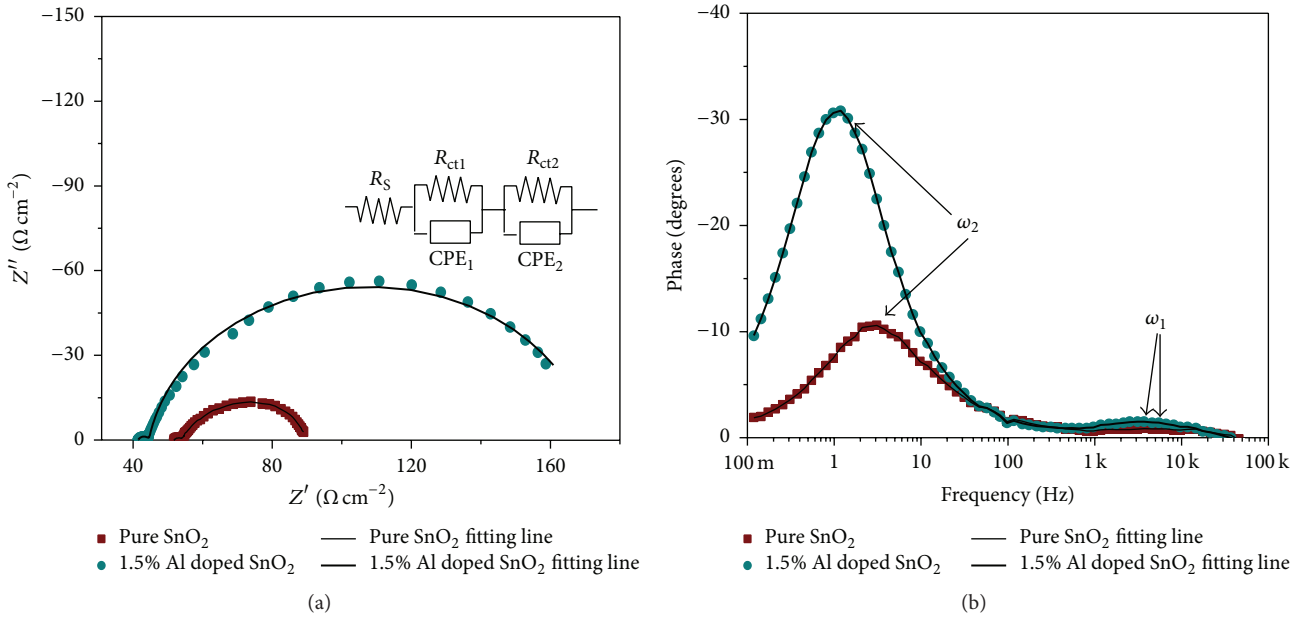

FIGURE 5: Nyquist plots (a) and Bode phase plots (b) of the DSCs based on the pure SnO_2 and 1.5% Al doped SnO_2 hollow microspheres.

lifetime of photoexcited electrons was lengthened. The total photoelectrical conversion efficiency was improved from 0.46% to 3.04% after Al doping.

Competing Interests

The authors declare that they have no competing interests.

Acknowledgments

This work was supported by the Natural Science Foundation of China (nos. 51304062, 21403056, and U1404202).

References

[1] W. Q. Wu, Y. F. Xu, H. S. Rao et al., "Multistack integration of three-dimensional hyperbranched anatase titania architectures for high-efficiency dye-sensitized solar cells," *Journal of the American Chemical Society*, vol. 136, no. 17, pp. 6437–6445, 2014.

[2] M. Lv, D. Zheng, M. Ye et al., "Optimized porous rutile TiO_2 nanorod arrays for enhancing the efficiency of dye-sensitized solar cells," *Energy & Environmental Science*, vol. 6, no. 5, pp. 1615–1622, 2013.

[3] K. Kakiage, Y. Aoyama, T. Yano, K. Oya, J.-I. Fujisawa, and M. Hanaya, "Highly-efficient dye-sensitized solar cells with collaborative sensitization by silyl-anchor and carboxy-anchor dyes," *Chemical Communications*, vol. 51, no. 88, pp. 15894–15897, 2015.

[4] Z. M. Jarzebski and J. P. Marton, "Physical properties of SnO_2 materials I. Preparation and defect structure," *Journal of the Electrochemical Society*, vol. 123, no. 7, pp. C199–C205, 1976.

[5] E. Hendry, M. Koeberg, B. O'Regan, and M. Bonn, "Local field effects on electron transport in nanostructured TiO_2 revealed by terahertz spectroscopy," *Nano Letters*, vol. 6, no. 4, pp. 755–759, 2006.

[6] Y. D. Duan, J. X. Zheng, N. Q. Fu et al., "Enhancing the performance of dye-sensitized solar cells: doping SnO_2 photoanodes with Al to simultaneously improve conduction band and electron lifetime," *Journal of Materials Chemistry A*, vol. 3, no. 6, pp. 3066–3073, 2015.

[7] X. Li, Q. Yu, C. Yu et al., "Zinc-doped SnO_2 nanocrystals as photoanode materials for highly efficient dye-sensitized solar cells," *Journal of Materials Chemistry A*, vol. 3, no. 15, pp. 8076–8082, 2015.

[8] N. G. Park, M. G. Kang, K. S. Ryu et al., "Photovoltaic characteristics of dye-sensitized surface-modified nanocrystalline SnO_2 solar cells," *Journal of Photochemistry and Photobiology A: Chemistry*, vol. 161, no. 2-3, pp. 105–161, 2004.

[9] R. Dharmadasa, K. G. U. Wijayantha, and A. A. Tahir, "ZnO–SnO_2 composite anodes in extremely thin absorber layer (ETA) solar cells," *Journal of Electroanalytical Chemistry*, vol. 646, no. 1-2, pp. 124–132, 2010.

[10] S. J. Li, Y. Lin, Z. Chen et al., "Electrochemical impedance analysis of nanoporous TiO_2 electrode at low bias potential," *Chinese Chemical Letters*, vol. 21, no. 8, pp. 959–962, 2010.

[11] F. Fabregat-Santiago, J. Bisquert, G. Garcia-Belmonte, G. Boschloo, and A. Hagfeldt, "Influence of electrolyte in transport and recombination in dye-sensitized solar cells studied by impedance spectroscopy," *Solar Energy Materials and Solar Cells*, vol. 87, no. 1–4, pp. 117–131, 2005.